JOURNAL OF CATALYSIS **114**, 207–216 (1988)

Steady-State Kinetics of the Catalytic Reduction of Nitrogen Dioxide by Carbon Monoxide on Platinum

D. T. WICKHAM AND B. E. KOEL

Department of Chemistry and Biochemistry, and the Cooperative Institute for Research in Environmental Sciences (CIRES), University of Colorado, Boulder, Colorado 80309-0449

Received September 15, 1987; revised May 31, 1988

The steady-state kinetics of the reduction of nitrogen dioxide (NO_2) with carbon monoxide (CO) on a polycrystalline platinum foil have been investigated using reactant pressures between 1×10^{-7} and 5×10^{-6} Torr. At temperatures less than 400 K, the primary products formed are carbon dioxide (CO_2) and nitric oxide (NO). The CO_2 formation rate at temperatures less than 400 K is at least an order of magnitude greater for this reaction than for those of either CO + O_2 or CO + NO under similar reaction conditions. The reaction rate is first-order in CO pressure when $P_{CO}/P_{NO_2} < 0.25$ and first-order in NO_2 pressure when $P_{CO}/P_{NO_2} > 1$. The activation energy when $P_{CO}/P_{NO_2} = 0.10$ is 7.2 kcal mole^{-1} which is consistent with the activation energy for CO + O_2 under similar conditions. However, when $P_{CO}/P_{NO_2} = 1.5$, the activation energy is only 4.3 kcal mole^{-1}. This value is 29 kcal mole^{-1} lower than the activation energy for CO + O_2 at low temperatures when the reaction is first-order in the oxidant. Consistent reaction mechanisms for both regimes are proposed based upon recent reports of the chemisorption of NO_2 on Pt surfaces.

INTRODUCTION

The catalytic reduction of nitrogen dioxide (NO_2) by carbon monoxide (CO),

$$NO_2 + CO \rightarrow CO_2 + NO, \quad (1)$$

is being studied as a part of an effort to understand the reactions of nitrogen oxides (NO_x) on transition metal surfaces. These are interesting chemical systems and are important in several commerical applications. One application that currently is having a substantial impact in the fields of atmospheric and analytical chemistry results from the extremely sensitive chemiluminescence detection of NO. This has led to the development of techniques utilizing reaction (1) that allow quantitative determinations of trace (ppb) levels of NO_2 (*1, 2*) and CO (*3–5*). Additionally, federal laws which have emphasized reducing NO_x and CO emissions from automobile exhausts have generated an increased interest in the development of exhaust catalysts which effectively promote the reaction between NO_x and CO to produce CO_2 and N_2 (*6*).

Reaction (1) is interesting from a fundamental point of view because more than one possible Langmuir–Hinshelwood mechanistic pathway exists. The reaction may occur via a dissociative NO_2 mechanism:

$$NO_{2(g)} \rightarrow NO_{(a)} + O_{(a)} \quad (2\text{-}1)$$

$$NO_{(a)} \rightarrow NO_{(g)} \quad (2\text{-}2)$$

$$CO_{(g)} \rightarrow CO_{(a)} \quad (2\text{-}3)$$

$$CO_{(a)} + O_{(a)} \rightarrow CO_{2(g)} \quad (2\text{-}4)$$

A bimolecular reaction between coadsorbed NO_2 and CO is also possible:

$$NO_{2(g)} \rightarrow NO_{2(a)} \quad (3\text{-}1)$$

$$CO_{(g)} \rightarrow CO_{(a)} \quad (3\text{-}2)$$

$$CO_{(a)} + NO_{2(a)} \rightarrow CO_{2(g)} + NO_{(g)} \quad (3\text{-}3)$$

Recent investigations of the adsorption of NO_2 on Pt(111) (*7, 8*) and Pt foil (*9*) show that NO_2 decomposes readily at elevated temperatures to produce $NO_{(a)}$ and $O_{(a)}$ and that $NO_{(a)}$ has a significant desorption rate at 350 K. These studies suggest that Eq. (2)

0021-9517/88 $3.00

may be a significant reaction pathway. In this case, step (2-4), which may be rate limiting, is identical to the rate-determining step, Eq. (4-3), in the reaction between CO and O_2:

$$CO_{(g)} \rightarrow CO_{(a)} \quad (4\text{-}1)$$

$$\tfrac{1}{2}\, O_{2(g)} \rightarrow O_{(a)} \quad (4\text{-}2)$$

$$CO_{(a)} + O_{(a)} \rightarrow CO_{2(g)} \quad (4\text{-}3)$$

Therefore, the kinetics of NO_2 reduction may be similar to those observed for the CO + O_2 reaction if Eq. (2) represents a significant pathway. One additional complication that Eq. (2) contains is the possible inhibition of the reaction by the NO product.

Chemisorption studies (*7–9*) also report a reversibly adsorbed, molecular NO_2 state at low temperatures that may have a sufficient lifetime at reaction temperatures to be catalytically important. This suggests that the bimolecular mechanism, Eq. (3), may also contribute to the overall reaction rate.

Although the catalytic oxidation of CO with O_2 (*10–16*) and NO (*17–20*) has been studied extensively, no kinetic data for the reaction of CO with NO_2 on well-defined metal surfaces have been recorded. One early report which used a barium-promoted copper chromite catalyst is available (*21*), but changes in the chemical nature of the catalyst made it difficult to separate kinetic effects from changes in the catalyst activity or changes in reactant concentrations.

The objective of this investigation was to establish the kinetics of NO_2 reduction by CO over a clean platinum surface. We combined this information with previous detailed studies of NO_2 adsorption and desorption on Pt surfaces along with reported data for the oxidation of CO by O_2 and NO over Pt catalysts in order to gain insight into the reaction mechanism.

METHODS

The apparatus used to carry out the steady-state kinetic measurements is similar to that described previously by Golchet and White (*10, 22*). The 1.3-liter chamber was maintained at a base pressure of 5×10^{-9} Torr with a 60 liter s^{-1} ion pump attached to the chamber through a 1-in. gold seal valve that mechanically limited the pumping speed to a constant value. The total pressure of the system was monitored by a nude, Bayard-Alpert-type ionization gauge. Reactant and product partial pressures were measured with a Dycor quadrupole mass spectrometer, that was calibrated against the ion gauge taking into account the relative gauge sensitivities. The gauge sensitivity for NO_2 (S_{NO_2}/S_{N_2}) was calculated to be 0.17 based on tabulated ionization cross sections (*23*).

The polycrystalline platinum foil (99.998%, 1.48 cm × 1.51 cm × 0.1 mm) sample was suspended between two 3.2-mm tantalum support rods using 0.25-mm tantalum wire leads, that were spot-welded to both the support rods and the sample foil. The Pt sample was out of line-of-sight with any filaments in the chamber. The sample was resistively heated and the sample temperature was monitored with a Chromel–Alumel thermocouple, which was spot-welded to the center of the sample. An optical pyrometer was used to determine that no significant temperature variations (<30 K) existed on the foil when the sample was heated to temperatures exceeding 1000 K.

Research grade carbon monoxide (99.99% purity), electronic grade oxygen (99.998% purity), and reagent grade carbon dioxide (99.99% purity) supplied by Scientific Gas Products were used without further purification. Nitric oxide (Scientific Gas Products, C.P. grade, 99%) was purified by passing it through a silica gel trap cooled in a methanol/dry ice bath. High-purity NO_2 was prepared in our laboratory (*7*). Gases were introduced into the chamber from a high-pressure manifold through variable leak valves.

The platinum foil was pretreated by heating to 1050 K in 2×10^{-6} Torr O_2 for 15 h, followed by treatment at 1150 K in 2×10^{-6} Torr NO_2 for 4 h. In addition, the sample

was cleaned for approximately 30 min in 2×10^{-6} Torr NO_2 at 1150 K prior to each day's experiments. CO thermal desorption (TPD) was used to verify that the surface was free from contamination. After the above treatment, the CO TPD profile agreed well with those obtained by Winterbottom (*24*) and Collins and Spicer (*25*). The saturation coverage of CO at 300 K of 4×10^{14} molecules cm^{-2} as measured by TPD is also in good agreement with previous studies (*24*).

The rate of reaction (1) was assumed to be directly proportional to CO_2 pressure determined from the mass spectrometer signal at 44 amu. This relation would not hold if NO which is a product molecule in reaction (1) also reacts with CO to form N_2 and CO_2 as

$$NO + CO \rightarrow CO_2 + \tfrac{1}{2} N_2 \qquad (5)$$

Independent determination of the rate of reaction (5) by monitoring N_2 (28 amu) was not possible in our experiments because of the presence of CO (28 amu). However, Klein *et al.* (*19*) have derived an expression for the rate of reaction (5) on a platinum surface. Their model predicts that at the CO and NO_2 pressures studied here, the CO_2 production from reaction (5) would be significant only at temperatures in excess of 400 K. Our experiments verified this prediction. An additional interference may result from the formation of N_2O which has the same molecular weight as CO_2. Klein *et al.* (*19*) also have shown that the formation of this product on a platinum surface is a minor reaction for our conditions. Therefore, in this investigation, kinetic measurements were limited to temperatures less than 400 K, and as a result the CO_2 pressure above background is due only to reaction (1).

In all steady-state experiments, the desired conditions were set, the reaction was allowed to come to steady-state (usually less than 5 min), and the CO_2 pressure was obtained from the mass spectrometer. The background CO_2 pressure was determined by replacing the platinum foil with a 1.5-cm^2 sample of tantalum foil and then determining the CO_2 partial pressures corresponding to each reaction condition. During the background determinations, the rate of CO_2 formation was independent of the temperature of the tantalum foil, and therefore, no significant CO_2 production is attributed to this surface. Thus, in the steady-state experiments, The CO_2 background is due to wall or filament reactions rather than due to the sample support wires.

The CO steady-state coverage was obtained by allowing the reaction to reach steady state at the desired CO pressure (e.g., for $P_{NO_2} = 5 \times 10^{-6}$ Torr, $T = 350$ K) and then rapidly closing the CO leak valve while monitoring the CO_2 pressure. After approximately 10 s, the sample temperature was increased to 500 K and held there until no further CO_2 evolution was observed (no CO desorption was observed during the temperature ramp). The amount of CO_2 evolved during this procedure was calculated by integrating the CO_2 pressure versus time profile. The CO steady-state surface coverage can be calculated by assuming that all CO_2 was produced from the oxidation of adsorbed CO.

RESULTS

In Fig. 1, we show the total CO_2 production from NO_2 reduction over Pt at temperatures between 273 and 750 K. The CO_2 formation rate as turnover frequency (TOF) [molecules CO_2 (Pt atom)$^{-1}$ s^{-1}] and the 30 amu mass spectrometer signal (NO including, however, a significant contribution from NO_2 cracking) are plotted as functions of temperature for $P_{CO} = 1.5 \times 10^{-6}$ Torr and $P_{NO_2} = 1.0 \times 10^{-6}$ Torr. The CO_2 peak beginning at 450 K corresponds to the onset of CO_2 production from the CO + NO reaction, Eq. (5), as predicted by the model of Klein *et al.* (*19*). We also independently measured the rate for the NO + CO reaction and our studies agreed well with this model. The overall reaction rate decreases with increasing temperature above 600 K,

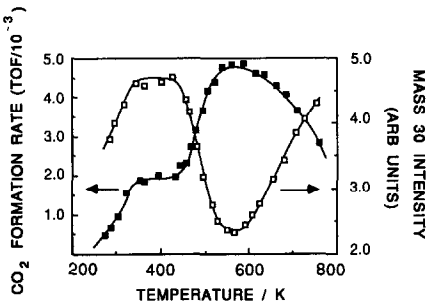

FIG. 1. CO_2 formation rate and mass 30 intensity for temperatures between 273 and 750 K at a CO pressure of 1.5×10^{-6} Torr and an NO_2 pressure of 1.0×10^{-6} Torr.

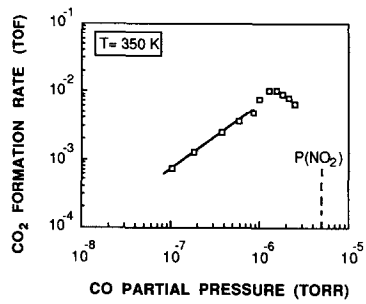

FIG. 2. CO_2 formation rate as a function of CO pressure at a fixed NO_2 pressure of 5×10^{-6} Torr at 350 K.

indicating a negative apparent activation energy in this temperature range.

Figure 1 also shows that the NO signal intensity parallels the CO_2 formation rate below 450 K but is opposite to the CO_2 formation rate above 450 K. This further confirms that the CO_2 formation is from reaction (1), in which NO is a product below 450 K. Only at temperatures exceeding 450 K does the rate of reaction (5), in which NO is a reactant, become significant.

Figure 2 shows a plot of reaction rate at 350 K versus CO pressure at a constant NO_2 pressure of 5×10^{-6} Torr. A linear regression analysis of the points up to a CO pressure of 9×10^{-7} Torr gives a slope of 0.94, which indicates that the reaction is first-order in CO pressure under these conditions. The rate constant is $6.7 \times 10^{+3}$ molecules CO_2 (Pt atom)$^{-1}$ s^{-1} (Torr CO)$^{-1}$ for this regime. When the CO pressure exceeds 1.3×10^{-6} Torr, the rate decreases showing that the reaction rate is inhibited by CO when P_{CO}/P_{NO_2} exceeds 0.25. Golchet and White (*10*) found for the reaction between O_2 + CO over platinum that the reaction rate was first-order in P_{CO} when $P_{CO}/P_{O_2} < 1$, but that the rate was not inhibited by CO until $P_{CO}/P_{O_2} > 1$. Finally, a small jump in the rate is observed at $P_{CO} = 9 \times 10^{-7}$ Torr, $P_{CO}/P_{NO_2} = 0.18$. When the experiment was repeated going from high to low CO pressures (opposite of the procedure used for Fig. 2), similar results were obtained. A possible explanation for this will be presented later.

In Fig. 3, the reaction rate at 350 K is plotted against NO_2 pressure at a constant CO pressure of 1.5×10^{-6} Torr. A linear regression analysis of the points up to an NO_2 pressure of 1.7×10^{-6} Torr yields a slope of 1.08. These results show that the reaction is first-order in NO_2 pressure under the conditions that the NO_2 pressure is less than or equal to the CO pressure. The rate constant for this regime is $4.4 \times 10^{+3}$ molecules CO_2 (Pt atom)$^{-1}$ s^{-1} (Torr NO_2)$^{-1}$. The reaction rate is weakly dependent upon NO_2 pressure as P_{NO_2}/P_{CO} exceeds 1 and as the ratio approaches 3, the reaction rate may be inhibited by larger NO_2 pressure although the effect is not as severe as was observed with CO.

The apparent activation energy of the re-

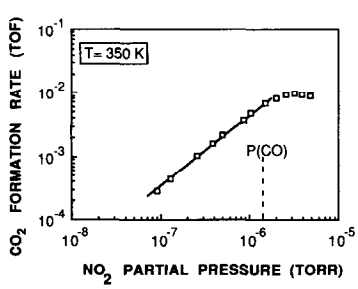

FIG. 3. CO_2 formation rate as a function of NO_2 pressure at a fixed CO pressure of 1.5×10^{-6} Torr at 350 K.

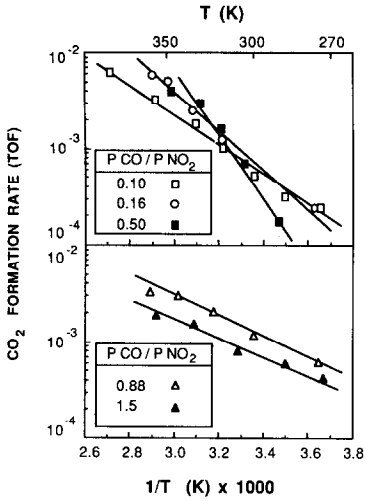

FIG. 4. Arrhenius plots for the following conditions: (top panel) $P_{CO}/P_{NO_2} = 0.10$ ($P_{CO} = 5.0 \times 10^{-7}$ Torr, $P_{NO_2} = 5.0 \times 10^{-6}$ Torr); $P_{CO}/P_{NO_2} = 0.16$ ($P_{CO} = 8.0 \times 10^{-7}$ Torr, $P_{NO_2} = 5.0 \times 10^{-6}$ Torr); $P_{CO}/P_{NO_2} = 0.50$ ($P_{CO} = 2.0 \times 10^{-6}$ Torr, $P_{NO_2} = 4.0 \times 10^{-6}$ Torr); (bottom panel) $P_{CO}/P_{NO_2} = 0.88$ ($P_{CO} = 1.5 \times 10^{-6}$ Torr, $P_{NO_2} = 1.7 \times 10^{-6}$ Torr); $P_{CO}/P_{NO_2} = 1.5$ ($P_{CO} = 1.5 \times 10^{-6}$ Torr, $P_{NO_2} = 1.0 \times 10^{-6}$ Torr).

action was determined for P_{CO}/P_{NO_2} values ranging from 0.10 to 1.5. The Arrhenius plots for $P_{CO}/P_{NO_2} = 0.10$, 0.16, and 0.50 are shown in the upper panel of Fig. 4. The slopes of these lines yield apparent activation energies of 7.2, 8.4, and 14 kcal mole^{-1}, respectively. These results agree well with those of Golchet and White (*10*) who obtained a value of 7.2 kcal mole^{-1} for $P_{CO}/P_{O_2} = 0.2$ over the temperature range of 450 to 530 K.

The Arrhenius plots for $P_{CO}/P_{NO_2} = 0.88$ and 1.5 are shown in the lower panel of Fig. 4. The slopes of these lines yield activation energies of 4.5 kcal mole^{-1} for $P_{CO}/P_{NO_2} = 0.88$ and 4.3 kcal mole^{-1} for $P_{CO}/P_{NO_2} = 1.5$. These results are quite different from the values reported for the platinum catalyzed CO + O_2 reaction under similar conditions. For $P_{CO}/P_{O_2} = 1$, Golchet (*26*) reports a value of 15 kcal mole^{-1}, and at $P_{CO}/P_{O_2} = 5$, White and Golchet (*22*) report a value of 33 kcal mole^{-1}. Thus, it can be concluded that at temperatures less than 450 K, the oxidation of CO with NO_2 has a significantly lower activation energy than the oxidation of CO with O_2 when the reaction is first-order in the oxidant.

The maximum rate in Fig. 4 at 350 K of 5×10^{-3} molecules CO_2 (Pt atom)$^{-1}$ s^{-1} was compared directly in our laboratory to the CO_2 formation rates for both the O_2 + CO and the NO + CO reactions at similar CO and oxidant pressures. At 350 K, reaction rates for both O_2 + CO and NO + CO were below our minimum detectable CO_2 formation rate of 2×10^{-4} molecules CO_2 (Pt atom)$^{-1}$ s^{-1}. These results show that when NO_2 is used to oxidize CO over platinum foil, the CO_2 formation rate is at least an order of magnitude greater than that when either NO or O_2 is used as the oxidant at 350 K.

The data in Fig. 4 are summarized in Fig. 5 where the apparent activation energies are plotted versus the value of P_{CO}/P_{NO_2}. This figure shows that as P_{CO}/P_{NO_2} increases from 0.10 to 0.50 the activation energy increases from 7.2 to 14 kcal mole^{-1}. When $P_{CO}/P_{NO_2} = 0.88$, the activation energy has declined to 4.5 kcal mole^{-1} and does not change significantly when $P_{CO}/P_{NO_2} = 1.5$.

In Fig. 6, the steady-state, fraction CO coverage is plotted against CO pressure at a constant NO_2 pressure of 5×10^{-6} Torr and a sample temperature of 350 K. The CO coverage is based on a saturation value of 4×10^{14} molecules cm^{-2}. This figure shows

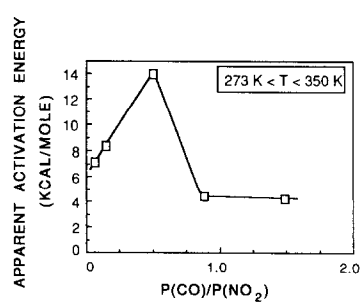

FIG. 5. Apparent activation energy as a function of P_{CO}/P_{NO_2} at reaction temperatures between 273 and 400 K.

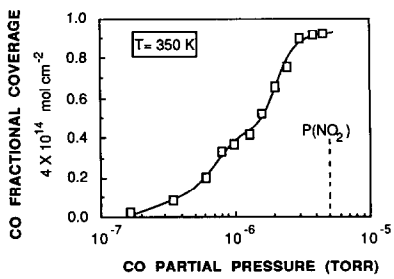

FIG. 6. Fractional CO coverage under steady-state reaction conditions as a function of CO pressure at a fixed NO_2 pressure of 5×10^{-6} Torr at 350 K.

that the CO coverage increases as the CO pressure increases for $P_{CO} < 3 \times 10^{-6}$ Torr and is near the saturation value when $P_{CO} = 3 \times 10^{-6}$ Torr. The CO coverage increases rapidly above $P_{CO} = 2 \times 10^{-6}$ Torr, $P_{CO}/P_{NO_2} = 0.4$, where the reaction order is negative with respect to CO pressure. This result is in good agreement with the results of Golchet and White (*10*) for the CO + O_2 reaction and also qualitatively agrees with a model for the CO + O_2 reaction proposed by Herz and Marin (*27*). Finally, a step or relatively flat portion of the curve is present (reproducibly) beginning at $P_{CO} = 9 \times 10^{-7}$ Torr, which corresponds to the CO pressure at which the jump in reaction rate was observed in Fig. 2. A possible explanation for both of these features will be presented later.

DISCUSSION

The discussion of these results is separated into two sections according to the ratio of P_{CO}/P_{NO_2}. The first section includes conditions where the $P_{CO}/P_{NO_2} \leq 0.50$ and the second section includes conditions where $P_{CO}/P_{NO_2} > 0.50$.

1. Kinetic Studies for $P_{CO}/P_{NO_2} \leq 0.50$

NO_2 has been shown to decompose to $NO_{(a)}$ and $O_{(a)}$ on clean Pt(111) (*7*) and on clean polycrystalline Pt surfaces (*9*) at temperatures above 170 K. Since NO desorbs readily from clean (111) and polycrystalline Pt surfaces at 350 K (*7, 9*) and oxygen does not desorb at an appreciable rate at this temperature, oxygen atoms are concentrated on the platinum surface when exposed to NO_2 at 350 K. Therefore, the reaction between NO_2 and CO under excess NO_2 conditions may occur via the dissociative mechanism shown in Eq. (2) and show kinetics similar to those observed for the CO + O_2 reaction under equivalent reactant pressures. This suggestion is supported by the activation energy obtained in this study of 7.2 kcal mole^{-1} for $P_{CO}/P_{NO_2} = 0.10$ which agrees well with the results of Golchet and White (*10*) for CO + O_2 under similar conditions.

The change in activation energy as a function of the P_{CO}/P_{NO_2} ratio can also be used to evaluate the proposed dissociative mechanism. As shown in Fig. 5, the activation energy increases from 7.2 to 14 kcal mole^{-1} as P_{CO}/P_{NO_2} is varied from 0.10 to 0.50. Figure 6 shows that the CO coverage increases significantly over this P_{CO}/P_{NO_2} range, and it is probable that the NO_2 or oxygen coverage (from NO_2 dissociation) decreases at the same time. The effects of adsorbed oxygen on the apparent activation energy of the CO + O_2 reaction on Pt(111) have been addressed by Campbell *et al.* (*12*). They suggest that increasing the oxygen coverage lowers the energy released upon adsorption for O_2 and CO which, in turn, decreases the activation energy of reaction. According to this model, the activation energy should increase with decreasing oxygen coverage or increasing P_{CO}/P_{NO_2}. This suggestion is consistent with the results presented in Fig. 5 for $P_{CO}/P_{NO_2} \leq 0.50$ and supports the proposed dissociative mechanism as the dominant pathway in this pressure regime.

In summary, the steady-state kinetic data for the catalytic reduction of NO_2 with CO obtained when $P_{CO}/P_{NO_2} \leq 0.50$ are similar to the data reported for the oxidation of CO with O_2 when the reaction is first-order in CO pressure (*10*). These results when combined with an understanding of the chemical nature of NO_2 adsorption on Pt surfaces

(*7, 9*) suggest that when $P_{CO}/P_{NO_2} \leq 0.50$, the dominant NO_2 reduction pathway is the dissociative mechanism shown in Eq. (2).

2. Kinetic Studies for $P_{CO}/P_{NO_2} > 0.50$

The activation energy for the reaction between NO_2 and CO when $P_{CO}/P_{NO_2} > 0.50$ was found to be less than 5 kcal mole^{-1}. For the CO + O_2 reaction at temperatures less than 500 K, the apparent activation energy is 33 kcal mole^{-1} when the reaction was first-order in O_2 pressure (*10*). It has been suggested for these conditions that the rate is limited by O_2 adsorption, which is inhibited by adsorbed CO molecules (*11*) and that the rate increase at high temperatures is a reflection of higher O_2 adsorption rates due to the thermal desorption of CO. Thus, the apparent activation energy of the reaction is the activation energy for CO desorption. The activation energy for CO desorption from a polycrystalline platinum surface is reported to be 25 to 32 kcal mole^{-1} (*25*), a range which is consistent with the apparent activation energy observed for the CO + O_2 reaction, but which is much higher than the activation energy reported here for the CO + NO_2 reaction. In addition, Fig. 1 shows that the CO_2 formation rate is relatively constant between 350 and 450 K, where the CO desorption rate is significant (*24*). These results show that for these conditions the reaction rate is not determined by NO_2 adsorption. This is not surprising, since the initial sticking coefficient for NO_2 is 0.9 at this temperature (*28*) and is not strongly affected by coverages less than 0.5 ML. By contrast, the initial sticking coefficient for O_2 is 0.05 and decreases rapidly with coverage (*29*).

In the absence of O_2 adsorption and dissociation limitations, the activation energy (E_{LH}) for the coadsorbed CO + O surface reaction on Pt(111) has been measured at 24 kcal mole^{-1} when Θ_O is low (*12*). Our results for the apparent activation energy of the CO + NO_2 reaction under similar conditions are approximately 19 kcal mole^{-1} lower than this value. Two possible explanations may account for this interesting observation.

First, the measured activation energy may not be a true measure of the activation energy for the surface reaction step. If the reaction is carried out under conditions in which the equilibrium concentration of the first-order reactant decreases as temperature is increased, the measured activation energy is given by

$$E_{app} = E_{LH} - E_d, \tag{6}$$

where E_{app} is the apparent activation energy measured experimentally, E_{LH} is the true activation energy of the surface reaction, and E_d is the activation energy of desorption for the first-order reactant, in our case NO_2 (*11*). Although TPD studies have shown that NO_2 has a significant desorption rate at high coverages in this temperature range (*7, 9*), the initial dissociative sticking coefficient for NO_2 only decreases from 0.96 to 0.92 on Pt(111) as the surface temperature is increased from 300 to 400 K (*28*). In addition, TPD studies have shown that oxygen atoms do not desorb from platinum at these temperatures (*30*) and that $NO_{(a)}$ and $O_{(a)}$ do not combined to form NO_2 (*7, 9*). Thus the coverage of oxygen atoms should not vary significantly with temperature under these reaction conditions, and therefore, Eq. (6) should not apply.

An alternative explanation for the low activation energy is that the dominant mechanistic pathway changes from Eq. (2) at $P_{CO}/P_{NO_2} < 0.50$ to a different pathway at $P_{CO}/P_{NO_2} > 0.50$. This change in mechanism may be the result of the high CO coverage which is present under these conditions as shown in Fig. 6. Coadsorbed oxygen has been shown to inhibit the dissociation of NO_2 on both Pt(111) and polycrystalline surfaces (*8, 9*) and adsorbed CO may have a similar effect. Thus, if NO_2 initially adsorbs onto a mostly CO-covered surface in an N-bonded nitro configuration as it does on an oxygen-covered Pt(111) surface (*8*), the coadsorbed CO molecules may inhibit the dissociation of NO_2 and effectively pro-

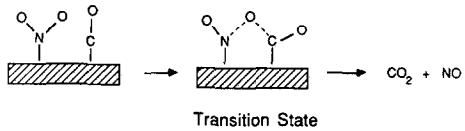

FIG. 7. Schematic diagram showing a possible bimolecular reaction between coadsorbed CO and NO_2 as shown in Eq. (3-3).

mote the bimolecular reaction between coadsorbed NO_2 and CO, Eq. (3-3), as shown in Fig. 7.

If the reactive sticking coefficient for NO_2 is assumed to remain relatively constant with temperature, as was the case for the dissociative sticking coefficient, then $E_{app} = E_{LH}$ and the activation energy of Eq. (3-3) is equal to 4.3 kcal mole^{-1}. This unusually low activation energy can be understood by comparing the strength of the bond which is broken in the transition state of this mechanism, the O–NO bond of adsorbed NO_2, to the strength of the bond broken in the transition state in Eq. (2-4), the O–Pt bond. The strength of the O–NO bond in the gas phase is 73 kcal mole^{-1} (*31*). We can estimate that this bond is further weakened upon adsorption by 20 kcal mole^{-1} (*32*) giving an O–NO bond energy in an N-bonded, adsorbed NO_2 molecule of approximately 53 kcal mole^{-1}. In contrast, the strength of the O–Pt bond which is broken in the transition state of Eqs. (2-4) or (4-3) is 83 kcal mole^{-1} (*30*). This difference in bond strengths of 30 kcal mole^{-1} suggests that the activation energy for Eq. (3-3) could be significantly less than the value of 24 kcal mole^{-1} observed for Eq. (4-3) and may approach zero, which is consistent with our results. Additionally, the proposed mechanistic change may be the cause of the jump in the reaction rate seen in Fig. 2 at $P_{CO} = 9 \times 10^{-7}$ Torr that also causes the flat portion of the CO steady-state coverage in Fig. 6 between $P_{CO} = 9 \times 10^{-7}$ and 1.5×10^{-6} Torr.

In Fig. 8, a potential energy diagram of the reaction between NO_2 and CO when $P_{CO}/P_{NO_2} = 1.5$ is compared to that for the reaction between O_2 and CO at low Θ_O. The potential energy scale was derived from heats of formation data. Heats of formation of the adsorbed species were calculated by subtracting the heat of adsorption from the heat of formation of the gas-phase species. Adsorption energies were calculated using the activation energies of desorption for each species adsorbed on Pt surfaces: 10 kcal mole^{-1} for NO_2 (*9*), 48 kcal mole^{-1} for O_2 (*30*), 25 kcal mole^{-1} for CO (*25*), 31 kcal mole^{-1} for NO (*9*), and 5 kcal mole^{-1} for CO_2 (*33*). Where multiple desorption states exist, the state most closely matching this steady-state condition was used. This figure shows that although the overall CO + NO_2 reaction is less exothermic than the CO + O_2 reaction by 14 kcal mole^{-1}, the surface CO + NO_2 reaction (adsorbed reactants going to adsorbed products) is more exothermic by approximately 30 kcal mole^{-1} than the surface CO + O_2 reaction. This large difference is due to the exothermicity associated with the formation of a stable adsorbed NO species.

In summary, the activation energy obtained in the steady-state kinetic analysis for conditions where $P_{CO}/P_{NO_2} > 0.50$ is approximately 19 kcal mole^{-1} less than the value obtained for the CO + O_2 reaction under similar conditions. We propose that under these conditions the reaction does not occur according to the dissociative

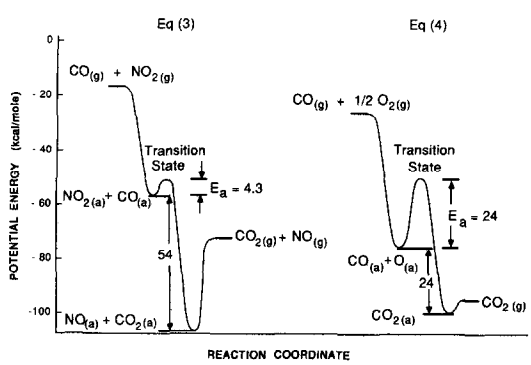

FIG. 8. Potential energy diagram comparing the bimolecular reaction between CO and NO_2 to the reaction between CO + $\frac{1}{2}$ O_2.

mechanism shown in Eq. (2), but occurs via the bimolecular pathway between coadsorbed NO_2 and CO shown in Eq. (3). Furthermore, we show how to account for the low (4.3 kcal mole^{-1}) activation energy for the bimolecular surface reaction.

CONCLUSIONS

Conditions have been identified under which the catalytic reduction of NO_2 with CO to form NO and CO_2, reaction (1), can be studied without interference from NO reduction, reaction (4). Steady-state kinetic measurements of reaction (1) have been made under these conditions. The reaction is first-order in CO pressure when $P_{CO}/P_{NO_2} < 0.25$ at 350 K. When $P_{CO}/P_{NO_2} > 0.25$ the reaction order becomes negative with respect to CO pressure. By contrast, the reaction is first-order in NO_2 pressure up to $P_{NO_2}/P_{CO} = 1.0$. The CO_2 formation rate at 350 K is at least an order of magnitude greater than that for either O_2 + CO or NO + CO under similar conditions.

As P_{CO}/P_{NO_2} increases from 0.10 to 0.50, the apparent activation rises from 7.2 to 14 kcal mole^{-1} which is consistent with a dissociative mechanism shown in Eq. (2). When P_{CO}/P_{NO_2} exceeds 0.50, the CO coverage approaches its saturation value of 0.25 ML and the apparent activation energy is very low, 4.3 kcal mole^{-1}. This is not consistent with the mechanism shown in Eq. (2), and we suggest that, under these conditions, the bimolecular mechanism shown in Eq. (3) predominates.

ACKNOWLEDGMENTS

Acknowledgement is made to the Donors of The Petroleum Research Fund, administered by the American Chemical Society for the support of this work, and to Barbara Banse for performing some of the experimental work. D.T.W. thanks the Cooperative Institute for Research in Environmental Sciences (CIRES) for providing a Visiting Fellowship.

REFERENCES

1. Bollinger, M. J., Sievers, R. E., Fahey, D. W., and Fehsenfeld, F. C., *Anal. Chem.* **55,** 1980 (1983).
2. Fahey, D. W., Eubank, C. S., Hubler, G., and Fehsenfeld, F. C., *J. Atmos. Chem.* **3,** 435 (1985).
3. Nyarady, S. A., Barkley, R. M., and Sievers, R. E., *Anal. Chem.* **57,** 2074 (1985).
4. Nyarady, S. A., and Sievers, R. E., *J. Amer. Chem. Soc.* **107,** 3726 (1985).
5. Sievers, R. E., Nyarady, S. A., Shearer, R. L., DeAngelis, J. J., Barkley, R. M., and Hutte, R. S., *J. Chromatogr.* **349,** 395 (1985).
6. Taylor, K. C., *Catal. Sci. Technol.* **5** (1984).
7. Bartram, M. E., Windham, R. G., and Koel, B. E., *Surf. Sci.* **184,** 57 (1987).
8. Bartram, M. E., Windham, R. G., and Koel, B. E., *Langmuir* **4,** 240 (1988).
9. Wickham, D. T., Banse, B., and Koel, B. E., submitted for publication.
10. Golchet, A., and White, J. M., *J. Catal.* **53,** 266 (1978).
11. Engel, T., and Ertl, G., "Advances in Catalysis" (D. D. Eley, P. W. Selwood, and P. B. Weisz, Eds.), Vol. 28, p. 1. Academic Press, New York, 1979.
12. Campbell, C. T., Ertl, G., Kuipers, H., and Segner, J., *J. Chem. Phys.* **73,** 5862 (1980).
13. Gland, J. L., and Kollin, E. B., *J. Chem. Phys.* **78,** 963 (1983).
14. Pacia, N., Cassuto, A., Pentenero, A., and Weber, B., *J. Catal.* **41,** 455 (1976).
15. Bonzel, H. P., and Ku, R., *J. Vac. Sci. Technol.* **9,** 663 (1972).
16. Barteau, M. A., Ko, E. J., and Madix, R. J., *Surf. Sci.* **104,** 161 (1981).
17. Hecker, W. C., and Bell, A. T., *J. Catal.* **84,** 200 (1983).
18. Lorimar, D., and Bell, A. T., *J. Catal.* **59,** 223 (1979).
19. Klein, R. L., Schwartz, S., and Schmidt, L. D., *J. Phys. Chem.* **89,** 4908 (1985).
20. Bolton, H., Hahn, T., LeRoux, J., and Lintz, H., *Surf. Sci.* **160,** L529 (1985).
21. Ayren, R. J., and Yonebayashi, T., *Atmos. Environ.* **1,** 307 (1967).
22. White, J. M., and Golchet, A., *J. Chem. Phys.* **66,** 5744 (1977).
23. Stephan, K., Helm, H., Kim, Y. B., Seykora, G., Ramler, J., Grossi, M., Mark, E., and Mark, T. P., *J. Chem. Phys.* **73,** 303 (1980).
24. Winterbottom, W. L., *Surf. Sci.* **37,** 195 (1973).
25. Collins, D. M., and Spicer, W. F., *Surf. Sci.* **69,** 85 (1977).
26. Golchet, A., Ph.D. thesis, University of Texas, 1973.
27. Herz, R. K., and Marin, S. P., *J. Catal.* **65,** 281 (1980).
28. Segner, J., Vielhaber, W., and Ertl, G., *Israel J. Chem.* **22,** 375 (1982).
29. Campbell, C. T., Ertl, G., Kuipers, H., and Segner, J., *Surf. Sci.* **107,** 220 (1981).

30. Gland, J. L., Sexton, B. A., and Fisher, G. B., *Surf. Sci.* **95,** 587 (1980).

31. Benson, S. W., "Thermochemical Kinetics." Wiley, New York, 1968.

32. This estimate comes from calculation of D(O–NO), the bond energy to dissociate either gas-phase NO_2 to $NO_{(g)} + O_{(g)}$ or adsorbed NO_2 to $NO_{(a)} + O_{(g)}$ using heats of formation data for gas-phase species from Benson (*31*) and heats of adsorption (*9*).

33. Matsushima, T., *Surf. Sci.* **127,** 403 (1983).